DISPERSION IN AN OPEN-CUT COAL MINE IN STABLY STRATIFIED FLOW

by

Clive Grainger[1]

Robert N. Meroney[2]

Prepared for Submission to

JOURNAL OF BOUNDARY LAYER METEOROLOGY

Fluid Mechanics and Wind Engineering Program
Civil Engineering Department
Colorado State University
Fort Collins, Colorado
80523

January 23, 1992

Revised May 22, 1992
Revised June 8, 1992

1 *Department of Mechanical Engineering, Monash University, Victoria, Australia*
2 *Department of Civil Engineering, Colorado State University, Colorado, USA*

CEP91-92CG-RNM-5

Table of Contents

DISPERSION IN AN OPEN-CUT COAL MINE IN STABLY STRATIFIED FLOW

by

Clive Grainger[1] and Robert N. Meroney[2]

[1] *Department of Mechanical Engineering, Monash University, Victoria, Australia*
[2] *Department of Civil Engineering, Colorado State University, CO, USA*

Abstract. Discharges from combustion within a coal pit which occur during night time inversion conditions may result in stagnant accumulation of smoke and dangerous gases which could inhibit mining operations. A wind-tunnel model study was performed to identify the range of flow and mixing conditions which could exist when stably stratified atmospheric surface flows pass over a large open pit. Flow penetration into the pit depended upon approach flow stability (Froude number) and the strength of thermal inversion within the coal pit. Measurements of wind speed and temperature were made upwind, within, and downwind of the pit. Concentration measurements were made within the pit of surface sources released along pit walls. Pollutant levels were found to be strong functions of the approach flow pit Froude number, source location, and release time.

1. INTRODUCTION

A terrace mining system has been proposed by the Electricity Trust of South Australia (ETSA) to mine the Leigh Creek coal field in South Australia. Once a minimum amount of overburden is removed above a coal seam all subsequent earth movement would be made along terraces by horizontally transporting unwanted earth above the unmined coal seam and dumping it on top of previously mined land (See Figure 1). This technique minimizes vertical transport of overburden; thus decreasing truck transport costs. The terracing system also reduces disturbance of unmined lands, automatically restores the overburden to surface mined regions, and limits the environmental impact of an open-pit mine operation.

After the loose overburden is dumped on the trailing terraces, residual coal and oil shale contained within the earth will combine with moisture resulting in spontaneous combustion generating dangerous fumes and smoke which ooze out of the overburden. Thus pollution sources may exist at various heights along the pit side walls, producing fumes of negligible buoyancy. Unless these combustion products are ventilated critical pollutants will rise over safe working limits.

A full safety analysis of the terrace mining concept must consider the full range of atmospheric conditions that can exist, the range of pit geometries and dimensions, the range and strength of possible smoke emissions, and the time scales associated with the diurnal cycle, weather conditions, and the combustion process. Windy conditions frequently associated with mildly-unstable and neutral atmospheric stability conditions (Pasquill Categories B, C, and D) should produce significant atmospheric mixing and coal-pit flushing conditions. Unstable

stratification (Pasquill Category A) will enhance dilution of coal-pit combustion products even during low winds. Concentration levels would reach maximum levels during stably stratified night-time situations, when mixing and flushing are minimal (Pasquill Category E, F and G).

When stably stratified surface flows are combined with night-time radiation surface cooling of the coal pit, surface flows may uncouple from the cooler air pooled within the excavation resulting in zero ventilation and continuous buildup of combustion products in the coal pit. Thus, this study focuses on stably stratified atmospheric conditions which are expected to produce critical pollutant levels. First, related studies of valley flows, nocturnal drainage flows in mountain basins, and the nature of mixing across inversions are examined. Second, insights provided by linear perturbation methods and numerical modeling are considered. Finally, measurements of wind speed, temperatures and dispersion over a 1:600 scale model of a generic coal pit are obtained.

a. Atmospheric processes over complex terrain

The stratified flows found over open-pit mines are expected to be similar to night-time drainage flows that develop over mountain basins due to accumulation of downslope cold air and nocturnal cooling. Most observations, analysis and research in this area have related to open-ended valleys of simple nocturnal slope winds where accumulation does not persist (Whiteman, 1990). The development of inversions above mountain basins begins in a similar manner to valley flows, but the inversion depth and strength tend to be stronger than those found over valleys or flat terrain (Maki *et al.*, 1986).

Typically, side wall drainage flow begins during early evening as the sun ceases to shine on one wall of the basin. This may well start a few hours earlier than the cooling at the bottom because of the topographic effect on the real sunset time. The cooler air accumulates at the bottom of the basin and joins air cooled through ground contact with soil which loses heat through radiation to the night sky. A still-calm layer develops to about 1/4 the depth of the valley, at which point the drainage flow begins to fill in on top of the pool of cold air (Maki and Harimaya, 1988; Whiteman, 1990).

Presuming a constant potential temperature profile exists as night falls, cooling results in the production of an inversion which grows upward until after about two to three hours the inversion reaches the local ridge top. The strength of the inversion is typically much stronger over a basin or valley than over flat terrain. The resulting temperature profiles are found to obey power-law relations with

$$\left[\frac{\theta(z,t) - \theta(h,t)}{\theta(h,t) - \theta(0,t)}\right] = -(1 - z/h)^a \qquad (1)$$

where z is height above the basin floor, h is basin depth and night time values of a equal to 1.75 over a valley versus values of 3.0 over a flat terrain (Maki and Harimaya, 1988).

Wind speeds over the basin tend to reduce the strength and height of any inversion. Indeed at ridge top speeds in excess of about 10 ms^{-1} the inversion may disappear. Maki *et al.*, 1986, and Manins and Sawford, 1982, both report that the presence or absence of an inversion seems to scale with a Froude number:

$$Fr = U_h[gh(\theta_h - \theta_o)/\theta]^{-\frac{1}{2}}, \tag{2}$$

where U_h is wind speed at valley ridge top, H_h is air temperature at ridge top, and H_o is temperature at valley floor level. When $Fr > 1.6$ then the basin inversion is swept away; when $1.3 > Fr > 1.6$ the air in the basin is coupled to air above the basin; and when $Fr < 1.3$ inversions form and the basin air is decoupled from the elevated flow. Magnitudes of this parameter appears to be independent of valley geometry.

Mountain meteorologists (Whiteman, 1990; McKee and O'Neal, 1989) like to describe valley and basin cross-sections in terms of a Topographical Amplification Factor (TAF) defined as:

$$TAF = [A_{xy}(h)/V_{valley}]/[A_{xy}(h)/V_{plain}], \tag{3}$$

where $A_{xy}(h)$ is the horizontal area through which energy enters or leaves the top of the volumes, V, at height $z = h$, and h is the height above the valley floor or plain. Thus the TAF emphasizes volumetric comparisons between a valley and the adjacent plain. The TAF characterizes the amount of trapped air under a given horizontal plane available to heat or cool as energy flux crosses the plane. Clearly a valley with less volume available beneath the top area will have a substantially larger diurnal temperature range. Thus it is found that a convex valley will produce stronger inversions than a U-shaped valley. This suggests that as a valley fills up with cold air and decreases it effective depth, the remaining air acts more like a flat plain situation. Typical values for the TAF are 2 for a V-notched valley, 1 for a box canyon, greater than 2 for convex bottom valleys, and between 1 and 2 for most other valley shapes.

For a trapezoidal shaped mountain basin or open-pit coal mine the TAF expression becomes:

$$TAF = 3\, W_1 B_1/[W_1 B_1 + W_2 B_2 + (W_1 B_1 W_2 B_2)^{1/2}], \tag{4}$$

where W and B are width and breadth, respectively, and subscripts 1 and 2 refer to top and bottom basin dimensions. Now TAF values vary between 1 and 3, and the value for a coal-pit shape similar to the proposed Leigh Creek dimensions would be 2.1. Hence, the air in the coal pit will cool down almost twice as fast as the air above the surrounding plain, resulting in strong inversions and cooler air in the pit.

b. Fluid Modeling of flow over complex terrain

Physical modeling studies of atmospheric flow over hills and mountains span 60 years of research. Dependent upon stratification, hill geometry and spacing various combinations of waves, downslope winds, valley penetration, streamwise division, upwind penetration, and blocking can be reproduced in the laboratory (Meroney, 1990). Measurements of isothermal boundary layers passing over sinusoidal boundaries were reported by Beebe (1972). Valley drainage flow situations have previously been simulated in wind tunnels by Hertig (1986) and Cermak and Petersen (1981).

Flow visualization experiments using valley models towed through salt-water have been completed at the Division of Atmospheric Research, CSIRO, Aspendale, Australia. Experiments by Bell and Thompson (1980) considered cross-flow over a sawtooth shape consisting of six crests and five troughs. More recently unpublished studies examined a single trough imbedded in a flat plain. These two-dimensional models show clearly the recirculation cell that occurs within the pit when a strong inversion caps the pit basin. As wind speed increases (Froude number increases) the inversion height lowers into the pit and more and more air is flushed out and downwind. Bell and Thompson found that sweeping flows always occurred over the sawtooth land forms when the Froude number exceeded 1.3. Similarly sweeping flows occurred over an isolated pit when the Froude number exceeded 1.2.[1]

Cunningham and Bedard (1992) examined the unsteady removal of inversion layers trapped in model mountain valleys. They measured the time-dependent decrease in inversion height as channel flow passed above dense salt water pools trapped between 2 model mountain ridges. Visualization identified several dynamic stages associated with the erosion of the inversions. Initially a starting vortex formed downwind of the valley. Next erosion occurs by entrainment at the top of the dense fluid, and Kelvin-Helmholtz waves briefly appear. During an intermediate stage the dense pool oscillates or sloshes while continuing to erode. During the final stage they observed that the inversion layer was driven up the lee of the upstream mountain and ventilated via a standing eddy.

2. PERTURBATION AND NUMERICAL MODELS FOR PIT AND VALLEY FLOWS

The circulation within a large open-pit coal mine for stable night time flows are similar to circulations which develop in valleys with cross-valley synoptic winds. Gross features of the flow field will be similar to those predicted by small amplitude methods and computational fluid mechanics models.

---

[1] For definition of "sweeping" proposed by Bell and Thompson (1980) see Section 2b.

a. Linear Perturbation Models for Cross-valley flows

When a flow of constant velocity, U, and constant vertical stratification, N (constant Brunt-Väisälä frequency), flows over a narrow pit of half width ,a, such that $a << U/N$, then linear perturbation theory predicts that dominant wavenumbers are greater than N/U, and the pit valley forces primarily evanescent waves which decay with height (See Figure 2a-A). But for a wide pit of finite depth such that $a >> U/N$, then the dominant wavenumbers are less than N/U, and waves propagate vertically with lines of constant phase tilting upstream. The wide open-pit mine limit is equivalent to the hydrostatic limit; hence it eliminates the dependence of vertical structure on the horizontal wave number. The pit profile will be reproduced at every level that is an integral multiple of $2\pi U/N$ (See Figure 2a-B). The linear perturbation solutions are identical to those produced by an isolated mountain of similar profile (See Duran (1990), Fig. 4.3b), but beginning at one-half the vertical wave length. Of course this simple solution is for inviscid flow with a slip boundary condition at the lower surface, constant vertical stratification and no horizontal temperature variations. Given a multi-layer stratification condition cross-flow over a large open-pit mine might even produce elevated waves, rotors and other mountain flow characteristics!

Tang (1976) extended the linear perturbation approach to consider the joint effect of horizontal surface temperature variation and valley shape on cross-valley wind circulations. He obtained lower-order successive approximation solutions to spectral representations for both typical daytime and nighttime situations. The method provides a series of linear equations whose solutions may be superimposed. Tang assumed a sinusoidal terrain, a linear mean potential temperature distribution with height, constant eddy exchange coefficients with height, a horizontal streamfunction at the top boundary, and a sinusoidal surface temperature distribution. By appropriate selection of the sign of the surface temperature perturbation amplitude one can simulate daytime conditions (warm valley floor and cool ridge tops) or nighttime drainage flows (cool valley floor and warm ridge tops).

Solutions were developed for 500 m deep valleys separated by 4 km ridge tops, ridge top wind speeds of 5 m sec^{-1}, and surface temperature extremes of $\pm 5°$ C. The daytime flow conditions produced a separated cell on the upflow valley wall with upslope return flow just above the lee slope. On the windward slope the prevailing wind persisted (See Figure 2a-C). For the nighttime case the computation produced a separated cell over the windward slope, with downslope winds on both valley walls (See Figure 2a-D) . The conditions described correspond to a valley Froude number equal to about 0.05.

b. Numerical Predictions of Valley Ventilation

As in many other fields, explicit numerical simulation of thermally driven flow fields has contributed to the understanding of valley winds. Gill (1966) proposed a conceptual model of two-dimensional flow in a two-dimensional cavity with diffentially heated sidewalls. In the absence of an external cross flow, his calculations produced cellular motion which agreed with laboratory experiments.

Later Bell and Thompson (1980) examined a two-dimensional model valley to investigate when a cross-valley wind will sweep out an initial stable thermal stratification. They presumed a periodic topography to simplify inflow specifications, and the top of the model was a horizontal streamline representing an inversion. Initially a linear thermal stratification was prescribed, and the horizontal velocity was taken to be independent of depth. They solved the inviscid, incompressible, and Boussinesq form of the equations of motion in both their hydrostatic and nonhydrostatic formulations. Their numerical models employed finite differences on a staggered grid, second upwind flux form of the differences, and a third-order predictor-corrector scheme to follow time variations. The boundary layer to valley depth ratio, D/h, was varied from 1.375 to 10, the boundary layer to valley width ratio, D/L was varied by a factor of two, and the Froude number ranged from 0.26 to infinity (corresponding to no stratification).

Apparently valley width variation does not alter scaled results whenever the hydrostatic assumption is valid. In the atmosphere under stable conditions, Fr is usually O(1) or less and h/L is almost always less than 0.3, so that $(\mathrm{Fr}\ h/L)^2 < 0.1$, and the hydrostatic assumption is valid. Most of the model integrations reached a quasi-steady flow situation after one hour of model time, at which time the result could be confidently put into the category of stagnation (velocity near zero or any situation where there is a closed circulation cell near the valley floor) or sweeping (no stagnant or reversed flow). For a sweeping flow the flow pattern is very similar to a potential flow for a homogeneous fluid. For a stagnant situation the temperature and streamline contours are essentially horizontal. The depth of the stagnant fluid decreases as Fr increases, and sweeping flow exists above a critical value of $\mathrm{Fr} = 1.3$ when $D/H > 1.8$.

Herwehe (1984) used a two-dimensional finite-element hydrostatic Boussinesq model for incompressible viscous flow to calculate flow and fugitive dust movement from an idealized open-pit copper mine. Turbulent exchange was parameterized by diffusion coefficients that were an analytic function of height, wind shear and surface roughness. Neutral stratification flows were modeled for trapezoidally shaped pits that were 1800 m wide, and either 35 m or 350 m deep. The pit sidewall slope for the deeper pit was 35°. Large surface roughness was assumed within the pit; hence, vertical mixing was large, no separation was observed, and the streamlines swept parallel to the valley floor. Small particles were predicted to disperse downwind in a Gaussian plume pattern from sources within the pit.

3. PHYSICAL MODELING

There are three succinct reasons physical modeling retains its value in meteorological analysis of terrain flows. First, fluid modeling does some things much better than current analytic and numerical alternatives; *e.g.*, it provides realistic information about surface fluxes, separation, and three-dimensional flow interactions. Second, wind tunnels are in effect analog computers that have the advantage of near-infinitesimal resolution and near-infinite memory. A fluid modeling study employs real fluids not models of fluids. Hence the fluid model is implicitly nonhydrostatic, non-Boussinesq, compressible, and viscid. Third, the fluid model bridges the gap between the fluid mechanician's analytical or numerical models of turbulence and

dispersion and their application. Meroney (1990) provides an extended discussion of modeling limitations, similarity considerations, facilities, and insights obtained from specific studies of both neutral and stratified flow over complex terrain.

Simulation of the stably-stratified atmospheric boundary layer interacting with a large open-pit coal mine requires geometric similarity of topographic relief and surface roughness, dynamic similarity of inertial and buoyancy forces, and similarly distributed mean and turbulent upwind velocity and temperature profiles. Viscous and coriolis forces are not expected to dominate; hence, equivalence of model and prototype Rossby and Reynolds numbers are not required. For these experiments equivalence between approach flow bulk Richardson numbers, $Ri_B = [g(\Delta T/T)\Delta z/(\Delta U)]^2$, and valley Froude numbers, $Fr = [U_h/(gh(T_h - T_o)/T)^{0.5}]$, were sought.

Critical trapping of fumes and combustion products are anticipated to occur during nighttime stable flows; hence, approach flow conditions equivalent to Pasquill categories E and F (Ri_B = 0.014-0.062 and 0.062-0.090 or L_{mo} = 23-125 m and 13-23 m, respectively) are required. It is possible to estimate the near surface temperature gradients required to model E and F stability for different tunnel wind speeds based on Richardson number equality. For a 1:600 scale model a prototype 3.5 ms^{-1} speed at a height of 10 m would require a model wind speed of 0.5 ms^{-1} and a model temperature difference ΔT = 3-13 °C over a 35 mm height for Pasquill Category E conditions and a model temperature difference ΔT = 13-19 °C over the same height for Pasquill Category F conditions.

A range of valley stagnation and partial erosion conditions should occur if model Froude numbers vary between 0.5 to 1.5. Given a 0.5 ms^{-1} model wind speed above a 0.3 m deep model pit, then air temperature differences between the pit bottom and ridge must be $(T_h - T_o)$ = 100°C and 11°C, respectively.

4. EXPERIMENTAL CONFIGURATION

Conventionally, stable stratification in wind tunnels is simulated using cold tunnel floors and heated air. Such a configuration requires either floor refrigeration or the use of cryogenic temperature gases such as liquefied air or sublimated CO_2 from dry ice. Since the experiments were to be performed over a large model in the Monash Environmental Wind Tunnel (MEWT: 10 m wide x 7 m high x 40 m long), an inverted model arrangement was chosen, and all heating was provided by electrical resistors placed along a false wind-tunnel roof. Britter (1974) used a similar arrangement of roof-mounted heaters to study turbulence development in a density stratified boundary layer.

a. Model Open-pit Coal Mine and Boundary-layer Heating

A false ceiling 18 m long by 6 m wide was constructed to insert in the MEWT, Figure 3. The ceiling was made modularly from five 3.6 m by 6 m plates and placed 2.5 m above the tunnel floor. In the fourth plate from the entrance a 1:600 generically shaped model pit was constructed to simulate a coal pit similar in size to the 1800 m long x 1000 m wide x 200 m deep Leigh Creek operation, Figure 4. The lower surface of the false roof was covered with aluminum-foil wrapped insulation to reduce heat loss and thermal inertia. All joints between the five plates were taped to smooth intersections and remove leaks.

Heating to produce the stably stratified boundary layer was produced by twenty-four electrical heater elements. Each element was individually rated to 2 kW for a 240 volt potential, but were connected in various serial and parallel combinations. Twelve elements were placed in a vertical grid just downwind of the roof entrance, and twelve more elements were distributed downwind in four rows next to the roof to act as booster heaters. At the low velocities used (0.5 ms^{-1}) dissipation of about 9 kW occurred. This energy sufficed to heat a boundary layer 300 mm thick, which is from five to ten times the depth of the anticipated model-scale Monin-Obukhov stability length, L_{mo} = 30 - 60 mm. Once the wind speed and heater elements were turned on it took from 1 to 2 hours for the flow conditions to stabilize.

Five rows of electrical tape heaters were also adhered to the surface of the model pit as shown in Figure 4. Electrical current to these heaters was adjusted to produce a range of pit surface temperatures. Thus, the approach Richardson number and pit Froude number could be separately adjusted by controlling wind speed, heater element current and heater tape current.

b. Instrumentation

The low air velocities and high temperature differences required that special instrumentation be utilized to assure that measurements were not biased by radiation errors. Velocities were measured using a Thermal Systems Inc. Model 1650 temperature corrected hot-film anemometer. The measurement element was placed horizontal and perpendicular to the flow and moved vertically on a mobile traverse stand. From ten to twenty measurements were made at vertical stations located from 10 to 860 mm from the ceiling.

Temperatures were measured using an array of ten shielded thermocouples probes. Two probe arrays were placed on mobile traverse stands, which could be located beneath the selected measurement stations. Measurements were also made at locations from 10 to 860 mm from the ceiling. The shielded system was calibrated against aspirated heated air, and the system was found to be accurate within $\pm 0.5°C$.

Concentrations of helium/air tracer gas mixtures were measured using a mass-spectrometer system. The density of the source gas was adjusted to produce locally neutral buoyancy. Two configurations were tested: a) a source placed halfway down and at the center of the upwind wall and b) a source placed halfway up and at the center of the downwind wall,

Figure 5. The source gas was released from a 9.5 mm diameter hole at a local velocity of 0.24 ms^{-1}. Measurements were made at various locations in and downwind of the pit. Concentration measurements were performed for three situations: fully stagnant, partially stagnant (small pit separation region), and skimming.

After an initial period of flow visualization using a Rosco theatrical smoke generator, a total of eleven exploratory experiments were performed utilizing a range of wind speeds and pit temperatures. Subsequently ten additional experiments were performed during each of which fourteen vertical traverses of velocity and temperature were measured around and within the model pit. The Bulk Richardson number conditions studied ranged from 0.0 (neutral) to 0.090 (Pasquill F), and pit Froude numbers ranged from 0.10 to infinity (neutral).

5. FLOW AND CONCENTRATION PATTERNS IN THE OPEN-PIT COAL MINE

Flow visualization revealed that air flow over the open-pit ranged from fully stagnant situations to complete skimming, Figure 6. At a Froude number of 0.10-0.55 a strong inversion formed over the pit, wind speeds within the pit were negligible and the pit and boundary layer levels appeared uncoupled. As wind speeds increased (or pit temperatures decreased) the boundary layer penetrated deeper into the pit, and the stagnant layer diminished in depth, Fr = 0.55-0.90. Sometimes the smoke filled mixed layer over the pit appeared to contain Kelvin Helmoltz waves. (Also observed by Cunningham and Bedard, 1992). As the Froude number increased the approach flow penetrated down the side of the upwind pit wall, but then it rose above a stagnant eddy which clung to the downwind region of the pit wall and floor. When conditions permitted the Froude number to increase to 1.3-1.8 the boundary layer fully penetrated the entire pit and flushed all air downstream.

During the first eleven experiments the pit boundary was heated by varying current to the five strip heaters covered by thin metal strips screwed to the bottom of the model pit. Single traverses of temperature were made above the center of the pit for a sequence of seven different wind speeds ranging from 0.1 to 1.45 ms^{-1}, then four tests were run at a constant wind speed of 0.5 ms^{-1} while the pit surface temperature was reduced by decreasing the strip heater power. Figure 7 displays the temperature profile variation with increased wind speed as Froude number increases from 0.1 to 1.2. Note the progressive penetration of the boundary layer into the pit. A similar temperature profile exists within the pit capped by a strong inversion region. Although Maki and Hariyama (1988) reported a power-law exponent of 1.8 above a quiescent mountain basin; the cross-valley flow situation produces a profile beneath the inversion which falls between curves generated by exponents of 1.8 and 3.0, but does not seem to obey a specific power law.

When the pit surface temperature decreases for constant wind speeds a different set of temperature profiles are produced, Figure 8. In this case the capping inversion decreases rapidly, and the underlying power-law profile region disappears. Smoke released during these runs suggested a wave appears in the boundary flow over the pit, which increases its wavelength and penetrates further into the pit as the pit temperatures decrease (Froude number increases).

a. Streamlines and Isotherm Contours

Contour plots were prepared of streamline and temperature cross-sections for both longitudinal and lateral flow sections. Despite the three-dimensional shape of the pit (aspect ratio of Y/X = 2/3) streamlines and isotherms were predominately two-dimensional except close to the side walls. Figures 9 through 11 display streamline and isotherm contours for Froude numbers ranging from 0.62 to 1.77. Figures 12 and 13 display streamline and isotherm contours for equivalent lateral cross-sections. Flow penetration observed at the windward edge of the pit during visualization is observed in both streamline and isotherms. The strong inversion appears in the temperature contours as closely spaced isotherms, and the stagnant regions are observed to persist in the downwind portion of the pit.

b. Concentration Measurements

Concentrations will increase in the pit after initiation of the source or inception of the inversion condition. Eventually mean concentrations in the mine will stabilize at their maximum levels. A filling test was performed for stagnation conditions (Fr = 0.62), source located on the downwind face, and sampler located 5 mm above the center of the pit. Concentrations reached a steady value after about 600 seconds, which given a model scale of 1:600 and typical model and field temperatures is equivalent to a prototype time of about 10 hours.

Figure 14 displays concentration profiles developed within the pit for up and downwind sources and stagnation versus flushing conditions. During stagnation conditions pit concentrations are nearly uniform over the pit height away from the source; whereas upwind pit concentrations are negligible for a downwind source during flushing situations. Figure 15 displays concentration contours for the same situations.

6. DISCUSSION OF FLUID MODELING RESULTS

When pit Froude number is less than 0.5 streamfunction and temperature contours above the pit remain nearly horizontal with only a small wave like penetration along the upwind face as warm (cooler in the prototype situation) air drains up into the model pit. However, when pit Froude number lies between 0.6 to 1.2 the streamline deviations tend to propagate upward (downward in the prototype situation) into the stable capping boundary layer almost undiminished in amplitude. This appears to agree with the projections of linear perturbation theory discussed in Section 2b that also predict elevated waves when the product Fr (h/a) is much less than one.

Flow over the center of the pit is definitely two-dimensional despite the fact that the lateral dimension of the pit is only two-thirds the pit length. At smaller pit Froude numbers the planes of constant temperature are essentially horizontal within the pit. Even at larger pit Froude numbers when the boundary layer dips into the pit itself, lateral isotherms are horizontal over the central one-half pit width.

Motions within the pit at low pit Froude numbers were too stagnant to be noticeable during smoke visualization. Nonetheless concentration profiles and contours definitely show a preference toward downstream motion for sources released on the upwind face. At larger Froude numbers gases released from the downstream face source only penetrate upwind after extended times. This behavior agrees with the nightime behavior predicted by linear perturbation theory in Figures 2a-D and 2b-B as developed by Tang, 1976.

7. CONCLUSIONS

The intention of this experimental program was to evaluate fumigation and dispersion conditions which might occur within large open-pit mines during stable atmospheric conditions. A novel "upside-down" experimental apparatus was constructed to carry out a measurement program over simulated open-pit mines in a large wind tunnel. The general behavior of the flow was found to agree with previous atmospheric experience, salt-water drag tank models, linear perturbation analysis, and computational-fluid-dynamics models. Specifically, one can conclude from this experimental exercise that:

a. Coal pit dispersion under stably-stratified conditions is dominated by the buoyancy-inertia forces expressed by the pit Froude number. Fully stagnant flow occurs when $Fr < 0.5$, partially stagnant flow occurs when $Fr = 0.5\text{-}1.0$, and flushing occurs when $Fr > 1.3$.

b. Greater pit fumigation occurs when pollutant sources are located on the downwind face of the coal pit, where they can exhaust into the standing eddy located along the downwind wall and floor.

c. Filling times to maximum equilibrium concentrations for Leigh Creek size open-pit mines occurs within prototype times of 10 hours under fully stagnant conditions.

d. Wind tunnels are able to effectively model stably stratified flows with the "upside-down" heater technique. The flow conditions stabilize rapidly, and alternate flow conditions are easy to adjust.

Acknowledgements

The second author wishes to acknowledge support from the National Science Foundation Cooperative Agreement BCS-882154, CSU/TTU Cooperative Program in Wind Engineering. He also gratefully acknowledges fiscal assistance for lodging and travel provided by the Department of Mechanical Engineering while on study leave at Monash University.

References

Beebe, P.S.: 1972, "Turbulent Flow Over a Wavey Boundary," Ph.D. Dissertation, Department of Civil Engineering, Colorado State University, 113 pp. (also THEMIS Technical Report No. 16, June 1972).

Bell, R.C. and Thompson, R.O.R.Y.: 1980, "Valley ventilation by cross winds," J. Fluid Mech., Vol. 96, Part 4, pp. 757-767.

Britter, R.E.: 1974, "An Experiment on Turbulence in a Density Stratified Fluid," Ph.D. Thesis, Department of Mechanical Engineering, Monash University, Clayton, Victoria, Australia.

Cermak, J.E. and Petersen, R.A.: 1981, "Physical Modeling of downslope mountain wind and atmospheric dispersion," Proc. Fourth U.S. National Conference Wind Engineering Research, Seattle, Washington, 11 pp.

Cunningham, W.J. Jr. and Bedard, A.J. Jr.: 1992, "The Removal of Inversion Layers from Mountain Valleys by an Upper Level Flow: A Scale Model Study," 30th Aerospace Sciences Meeting, January 6-9, 1992, Reno, NV, AIAA paper No. 92-0288, 6 pp.

Durran, D.R.: 1990, "Mountain Waves and Dowslope Winds," Chapter 4 from Atmospheric Processes Over Complex Terrain, American Meteorological Society, Monograph Vol. 23, No. 45, pp. 59-81.

Gill, A. 1966, "The Boundary-Layer regime for convection in a rectangular cavity," J. Fluid Mechanics, Vol 26, pp. 515-536.

Hertig, J.A.: 1986, "Some aspects of exotic simulations," Proceedings Third International Workshop on Wind and Water Tunnel Modelling of Atmospheric Flow and Dispersion, Lausanne, Switzerland, pp. 233-247.

Herwehe, J.A.: 1984, "Numerical modeling of turbulent diffusion of fugitive dust from an idealized open-pit mine." M.S. Thesis in Department of Earth Sciences, (Advisor: E.S. Takle) Iowa State University, Ames, IA, 336 pp.

Maki, M., Harimaya, T. and Kikuchi, K.: 1986, "Heat Budget Studies on Nocturnal Cooling in a Basin," J. of Meteorological Society of Japan, Vol. 64, No. 5, pp. 727-740.

Maki, M. and Harimaya, T.: 1988, "The Effect of Advection and Accumulation of Downslope Cold Air on Nocturnal Cooling in Basins," J. of Meteorological Society of Japan, Vol. 66, No. 8, pp. 581-597.

McKee, T.B. and O'Neal, R.D.: 1989, "The Role of Valley Geometry and Energy Budget in the Formation of Nocturnal Valley Winds," J. of Applied Meteorology, Vol. 28,pp. 445-456.

Manins, P.C. and Sawford, B.L.: 1982. "Mesoscale observations of upstream blocking, "Quart. J. Royal Met. Soc., Vol. 108. pp. 427-434.

Meroney, R.N.: 1986, "Guideline for Fluid Modeling of Liquefied Natural Gas Cloud Dispersion, Volume II: Technical Support Document," Gas Research Institute Technical Report No. GRI 86/0102.2 (CSU Report No. CER84-85RNM-50b, xx pp.

Meroney, R.N.: 1990, "Fluid Dynamics of Flow over Hills/Mountains--Insights Obtained through Physical Modeling," Chapter 7 from Atmospheric Processes Over Complex Terrain, American Meteorological Society, Monograph Vol. 23, No. 45, pp. 145-172.

Tang, W.: 1976, "Theoretical Study of Cross-Valley Wind Circulation," Arch. Met. Geoph. Biokl., Ser. A, Vol. 25, pp. 1-18.

Whiteman, C.D.: 1990, "Mountain Meteorology," Chapter 1 from Atmospheric Processes Over Complex Terrain, American Meteorological Society Monograph Vol. 23, No. 45, pp. 1-42.

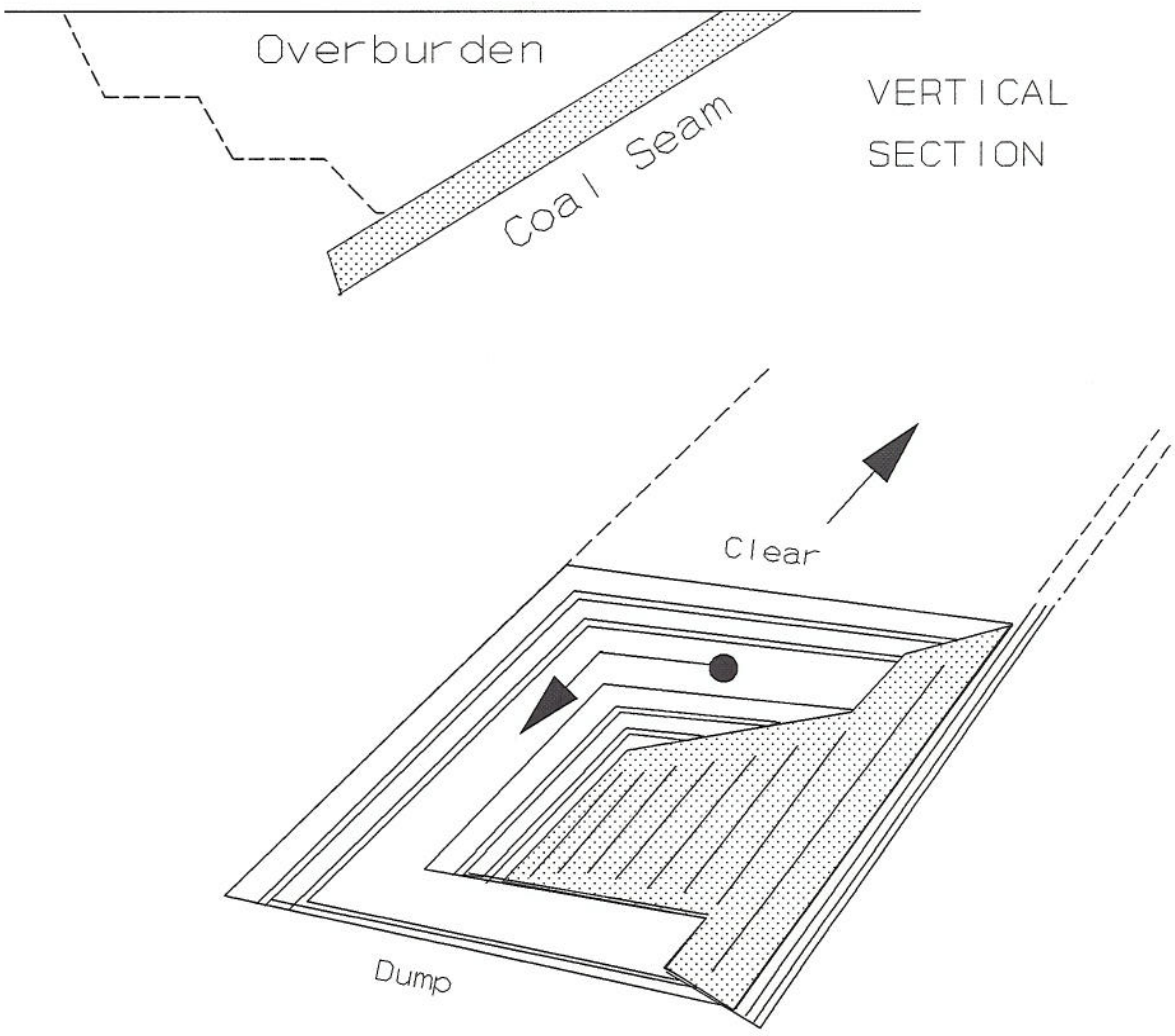

Fig. 1 Schematic of typical terrace-type open-pit coal mine. Typical dimensions: 1800 m long, 1000 m wide and 200 m deep.

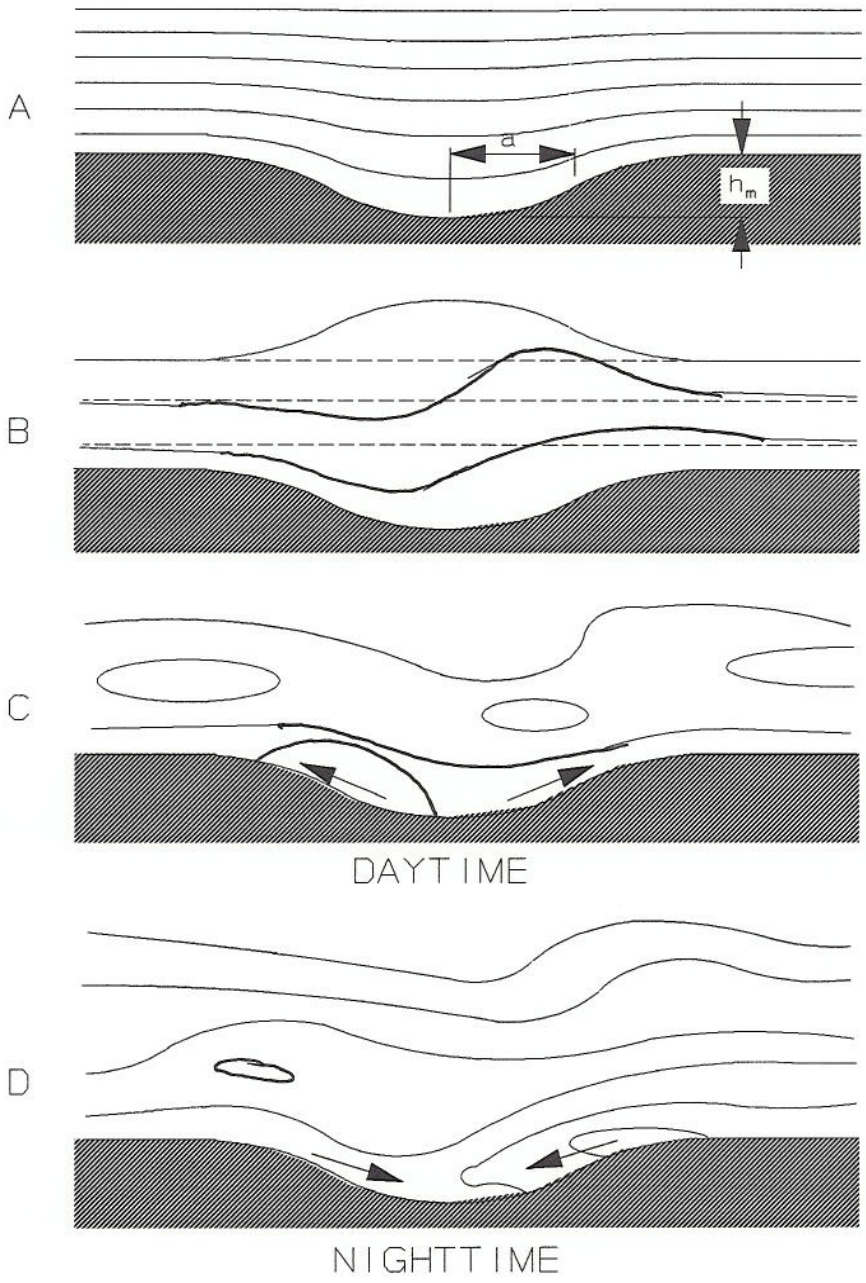

Fig. 2a Streamlines for airflow over an isolated bell-shaped valley when (A) a $<<$ U/N and (B) a $>>$ U/N given no surface heating versus cases where (c) a $>>$ U/N and valley temperatures are maximum or (D) minimum (Tang, 1976).

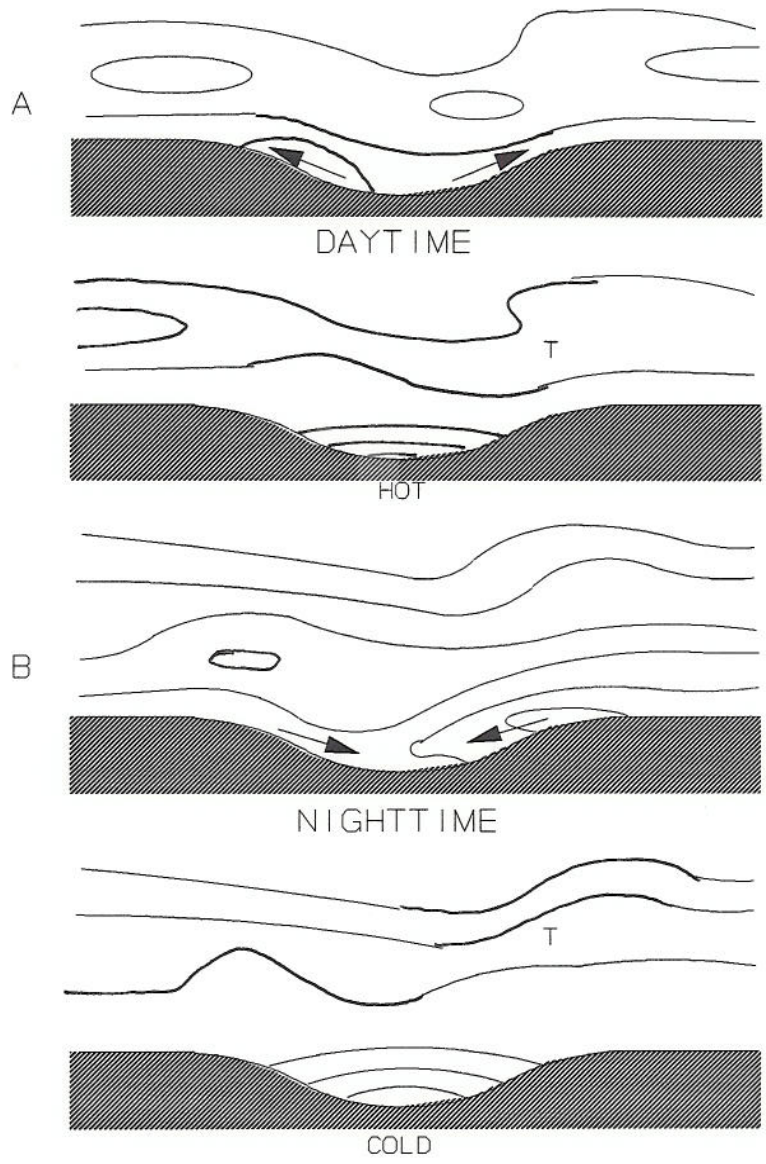

Fig. 2b Schematics of computed streamline and potential temperature fields (A) for the daytime case with prevailing cross valley wind, and (B) for the nighttime case with prevailing cross-valley wind (Tang, 1976).

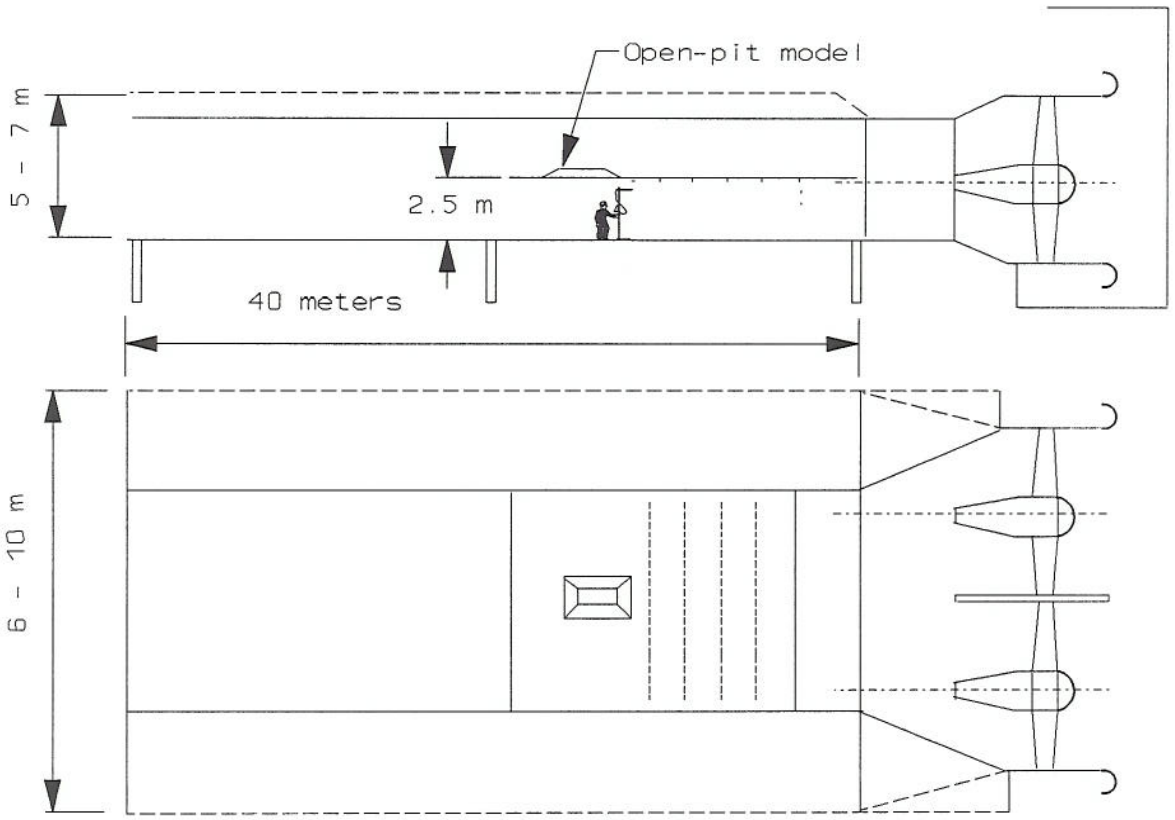

Fig. 3 Inverted open-pit mine model installed in Monash Environmental Wind Tunnel. All tests performed on lower false roof surface.

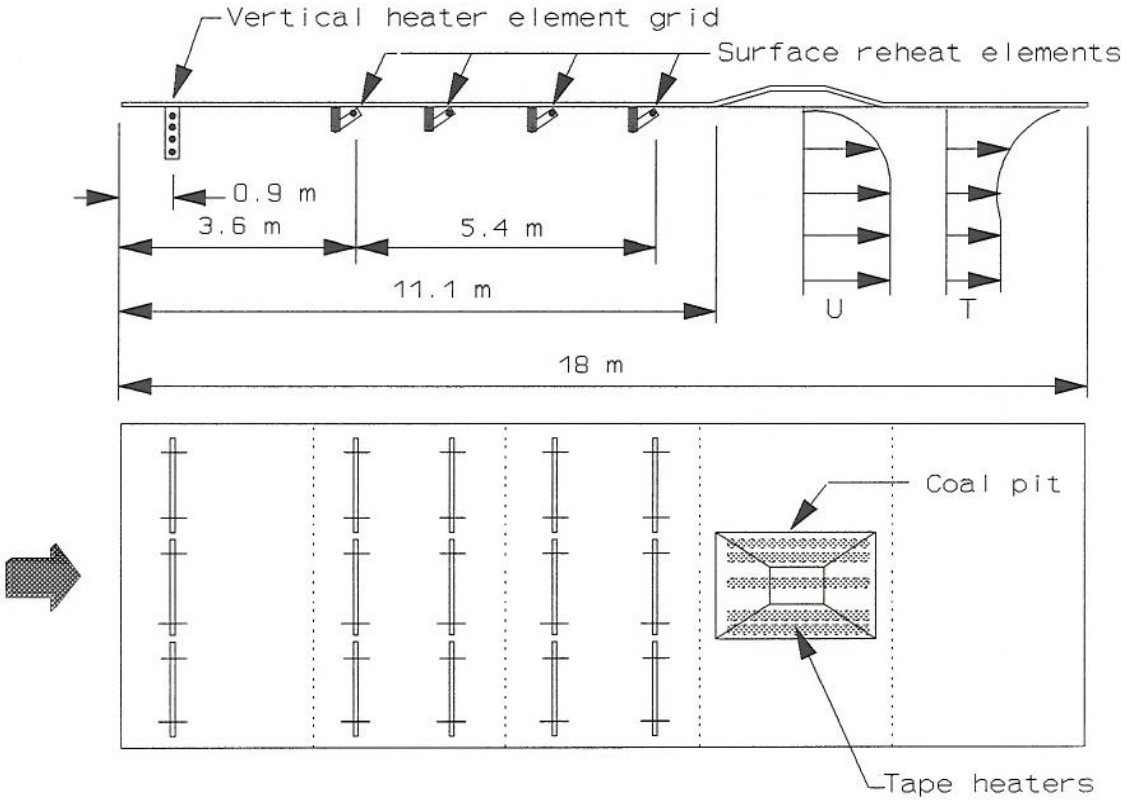

Fig. 4a Schematic of inverted-model open-pit coal mine configuration for insertion in the Monash Environmental Wind Tunnel. Twenty-four heater elements are each 2 m long @ 29 ohms or 2 kW capacity.

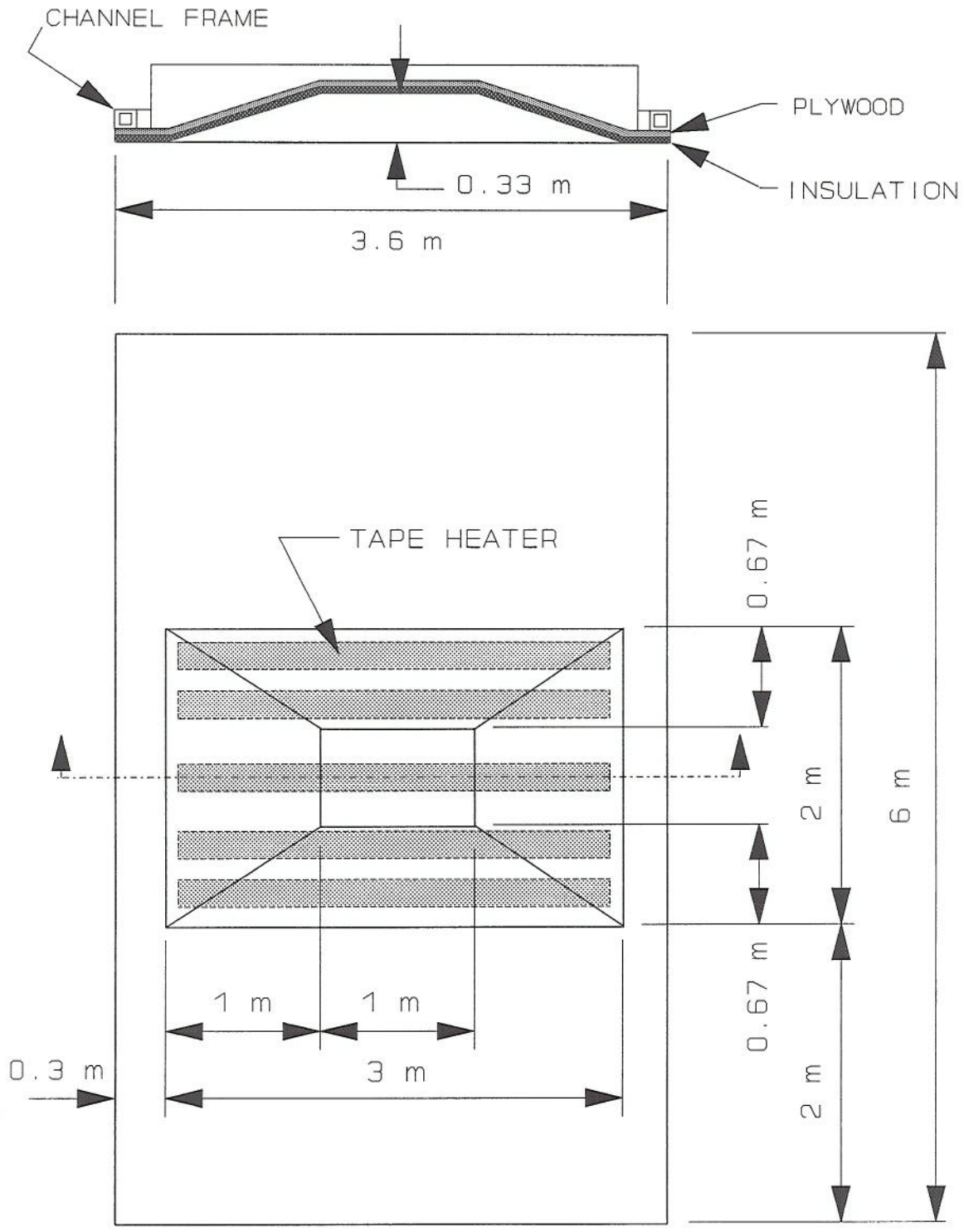

Fig. 4b Schematic of generic open-pit module for insertion in Monash Environmental Wind Tunnel. Five tape heaters are each 3 m long @ 150 Wm^{-1} or 450 W total.

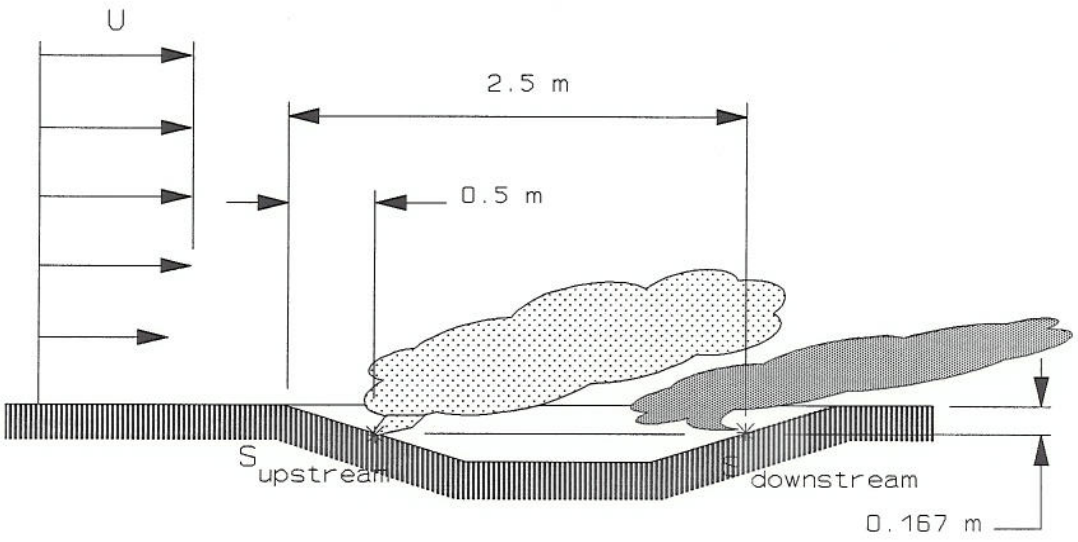

Fig. 5 Schematic of source locations in model open-pit. Helium/air mixture source gas was released from a 9.5 mm diameter hole at a local velocity of 0.24 ms^{-1}.

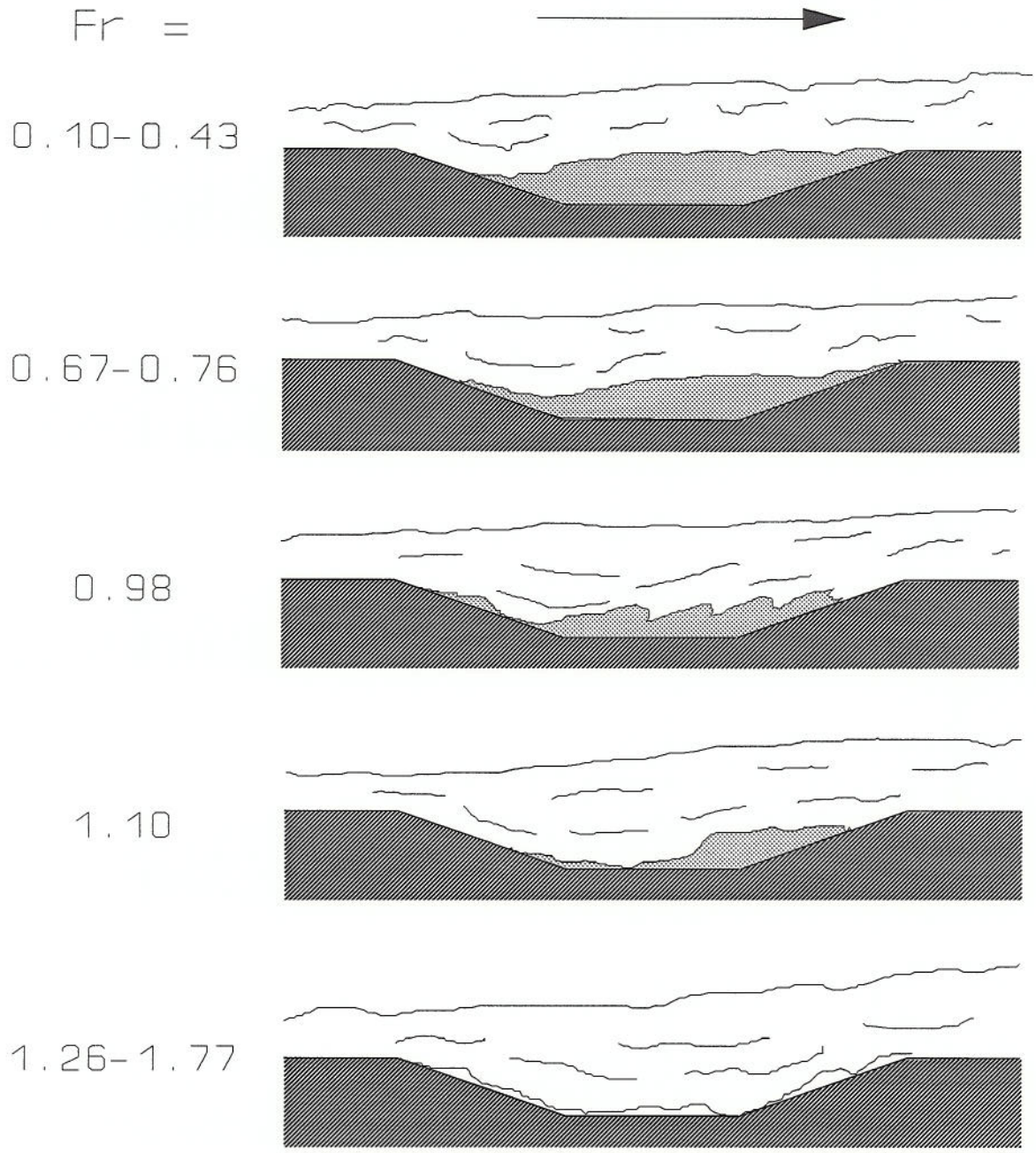

Fig. 6 Smoke appearance during sequence of visualizations of flow over model open-pit mine. As wind-tunnel speed increases from 0.1 to 1.45 ms^{-1} pit Froude number varies from 0.1 to 1.77.

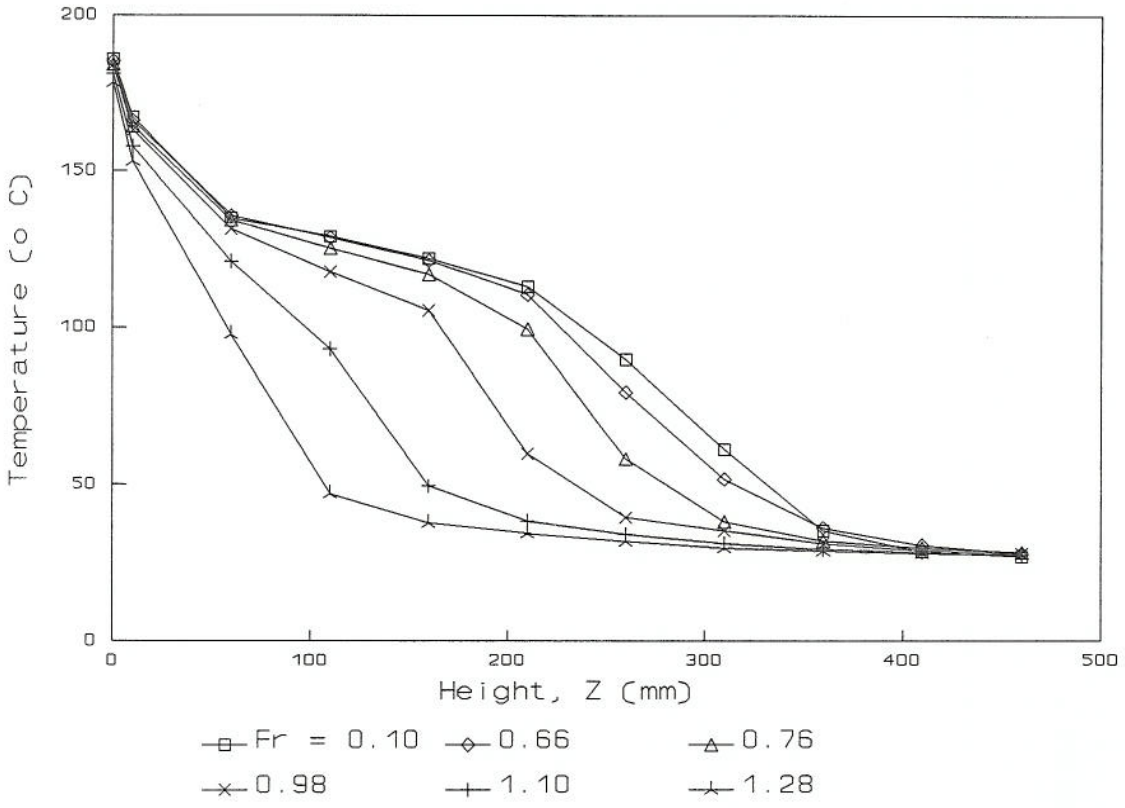

Fig. 7 Vertical profiles above center of model open-pit mine. As velocity increases from 0.10 to 1.45 ms^{-1} the pit Froude number varies from 0.10 to 1.28.

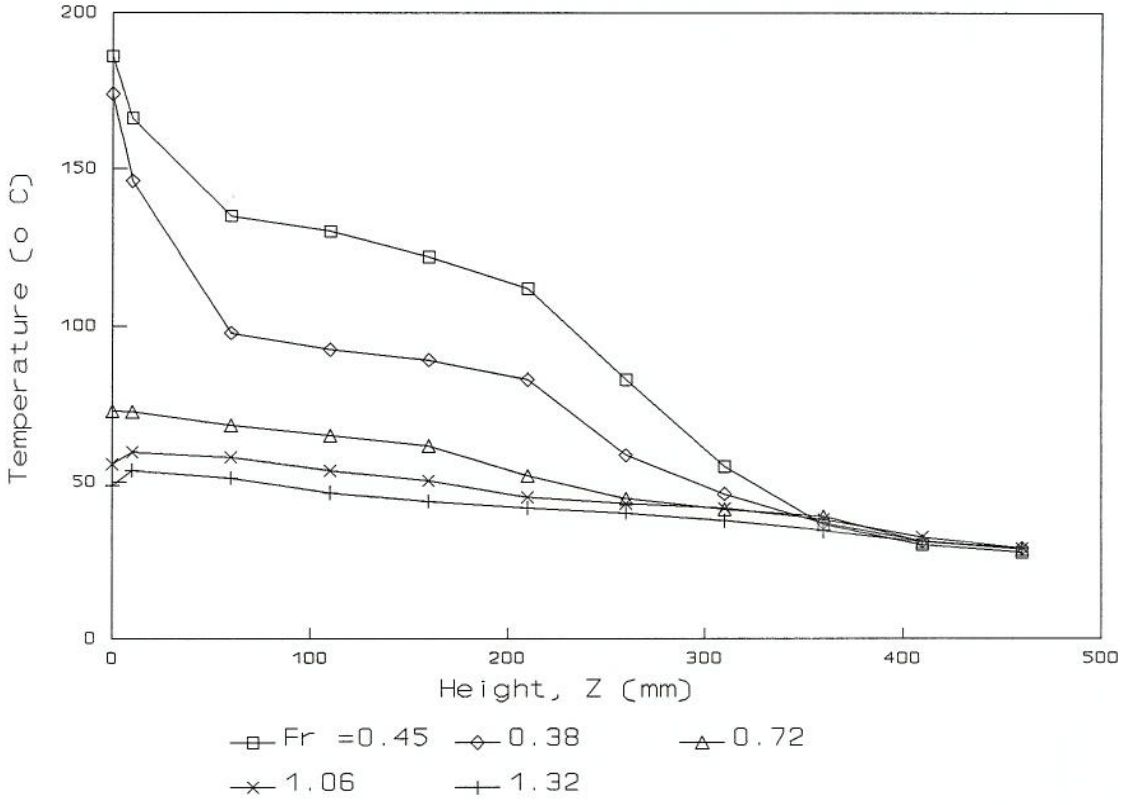

Fig. 8 Temperature profiles over center of open-pit model for constant wind speed and variable pit surface temperature. As pit temperature decreases from 186°C to 50°C the pit Froude number varies from 0.38 to 1.26.

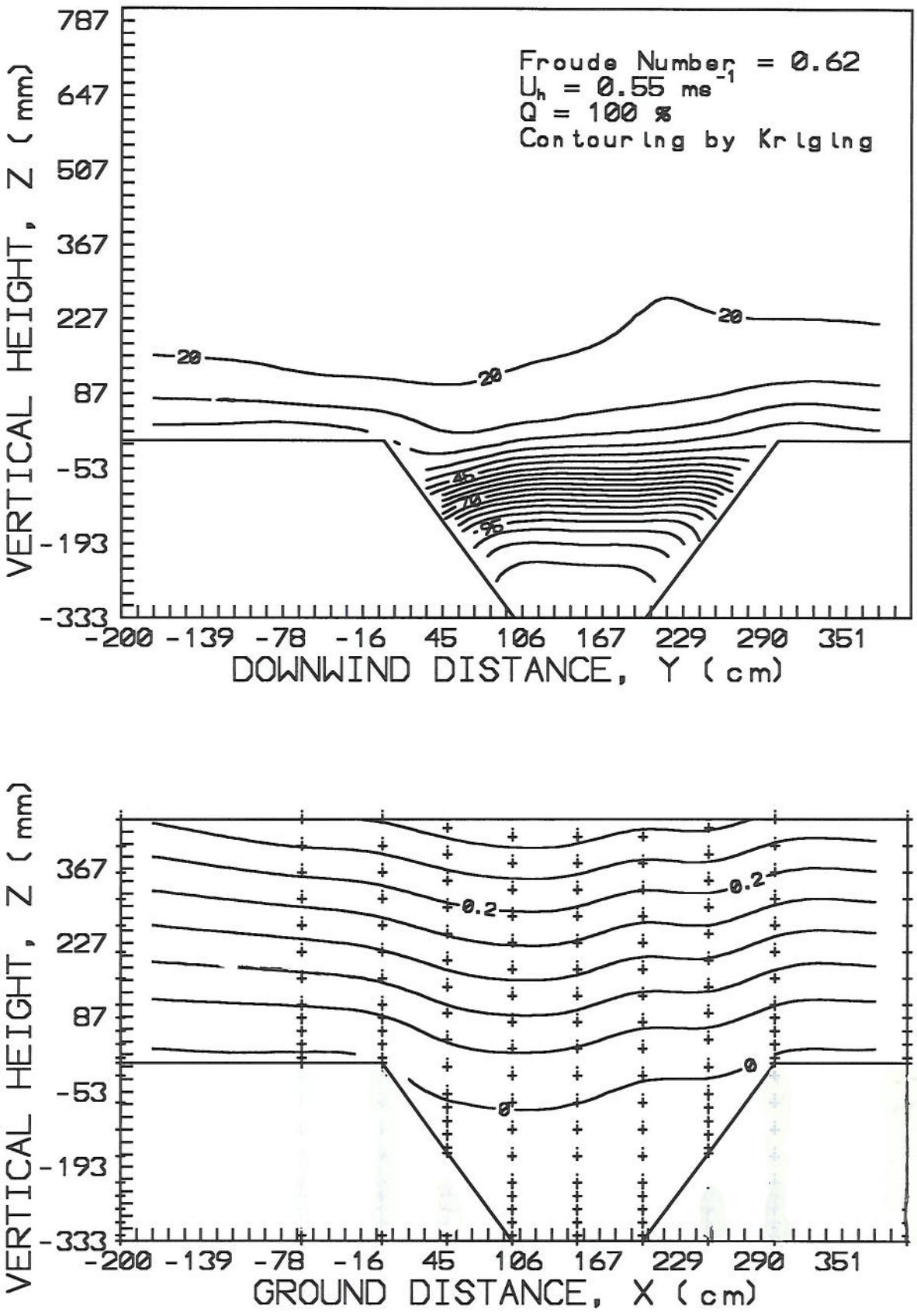

Fig. 9 Isotherms (°C) and streamline (m^2/s) contours over open-pit mine model. Fr = 0.62. Measurement locations noted by +.

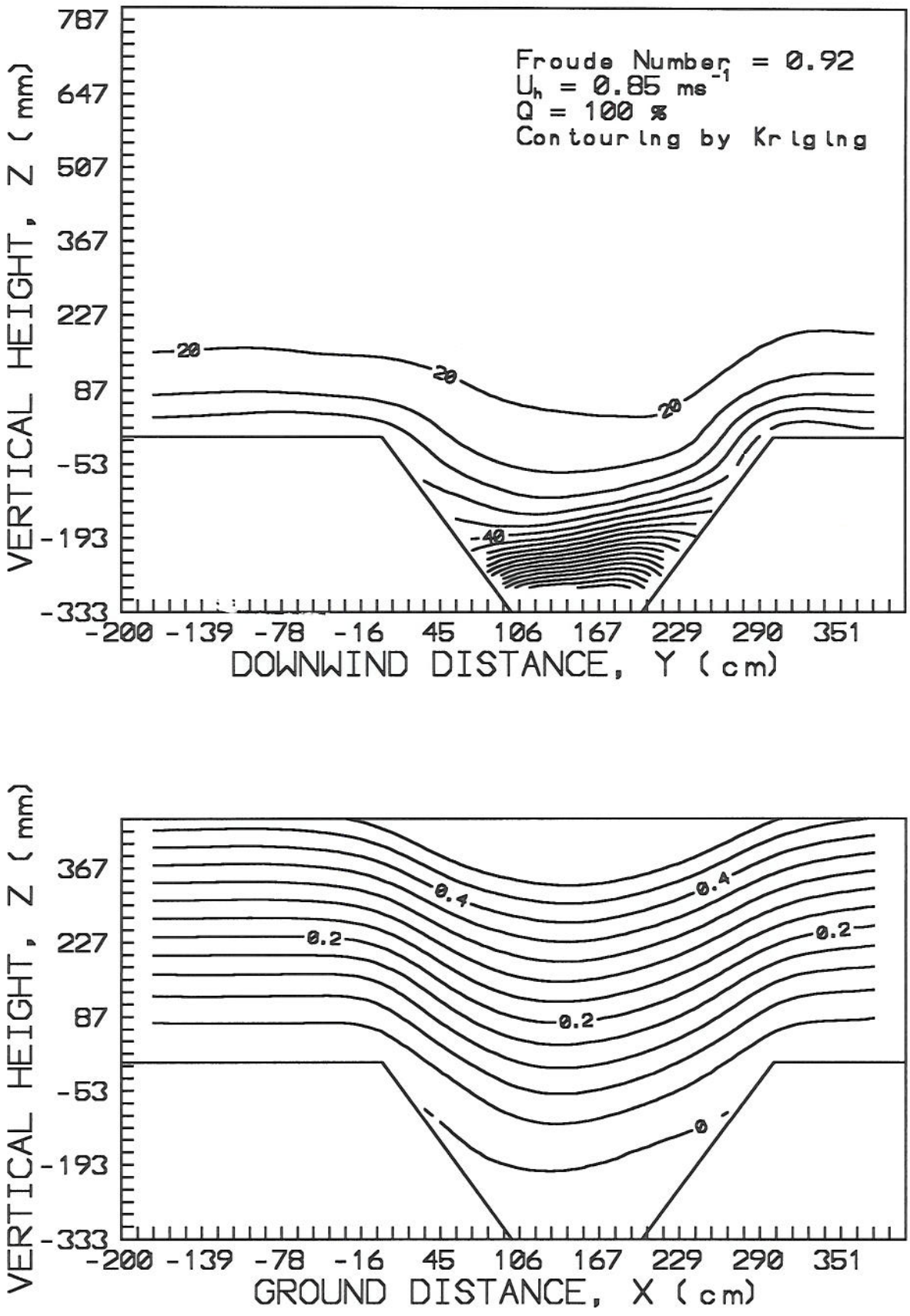

Fig. 10 Isotherms (°C) and streamline (m^2/s) contours over open-pit mine model. Fr = 0.92.

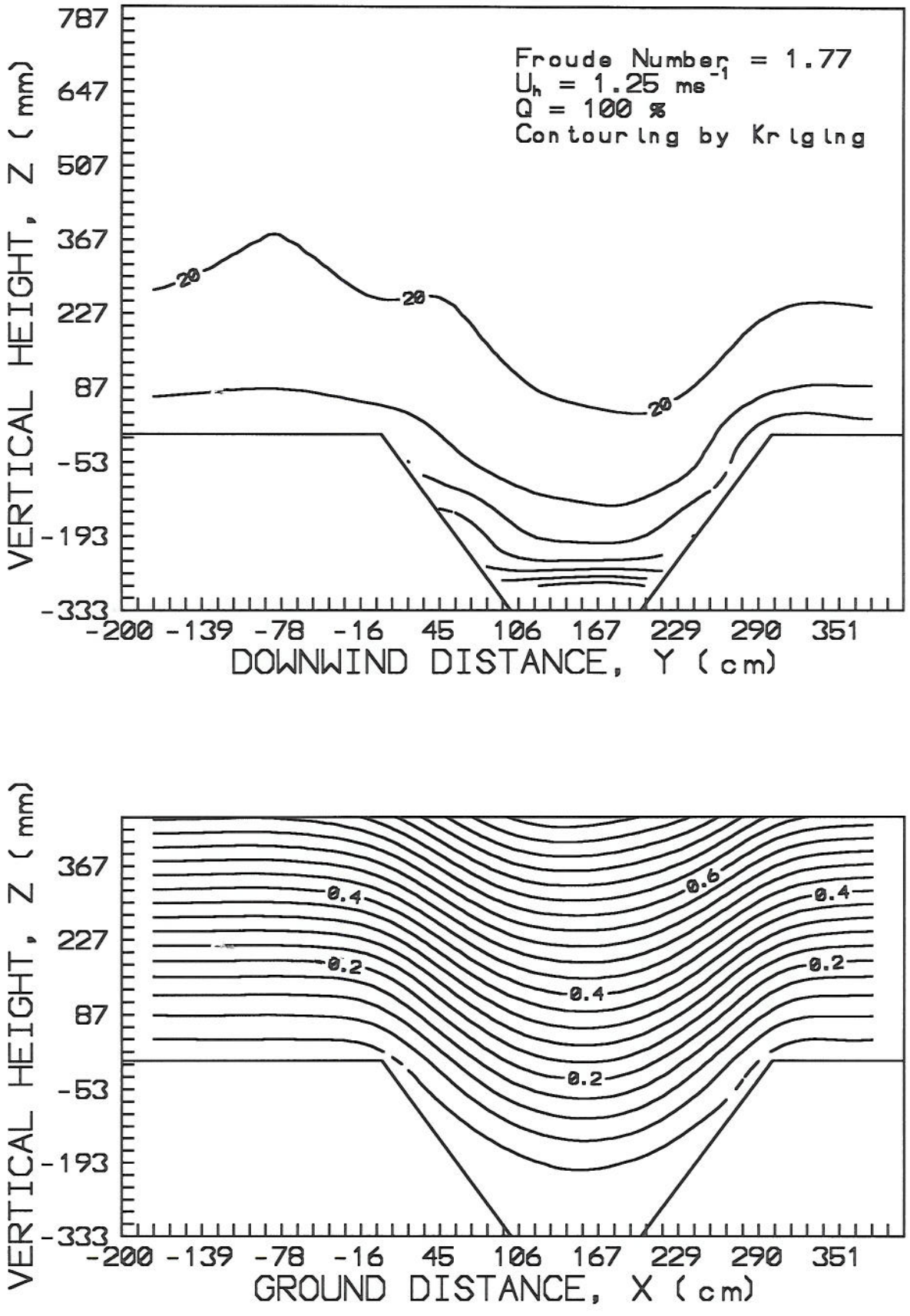

Fig. 11 Isotherms (°C) and streamline (m^2/s) contours above open-pit mine model. Fr = 1.77.

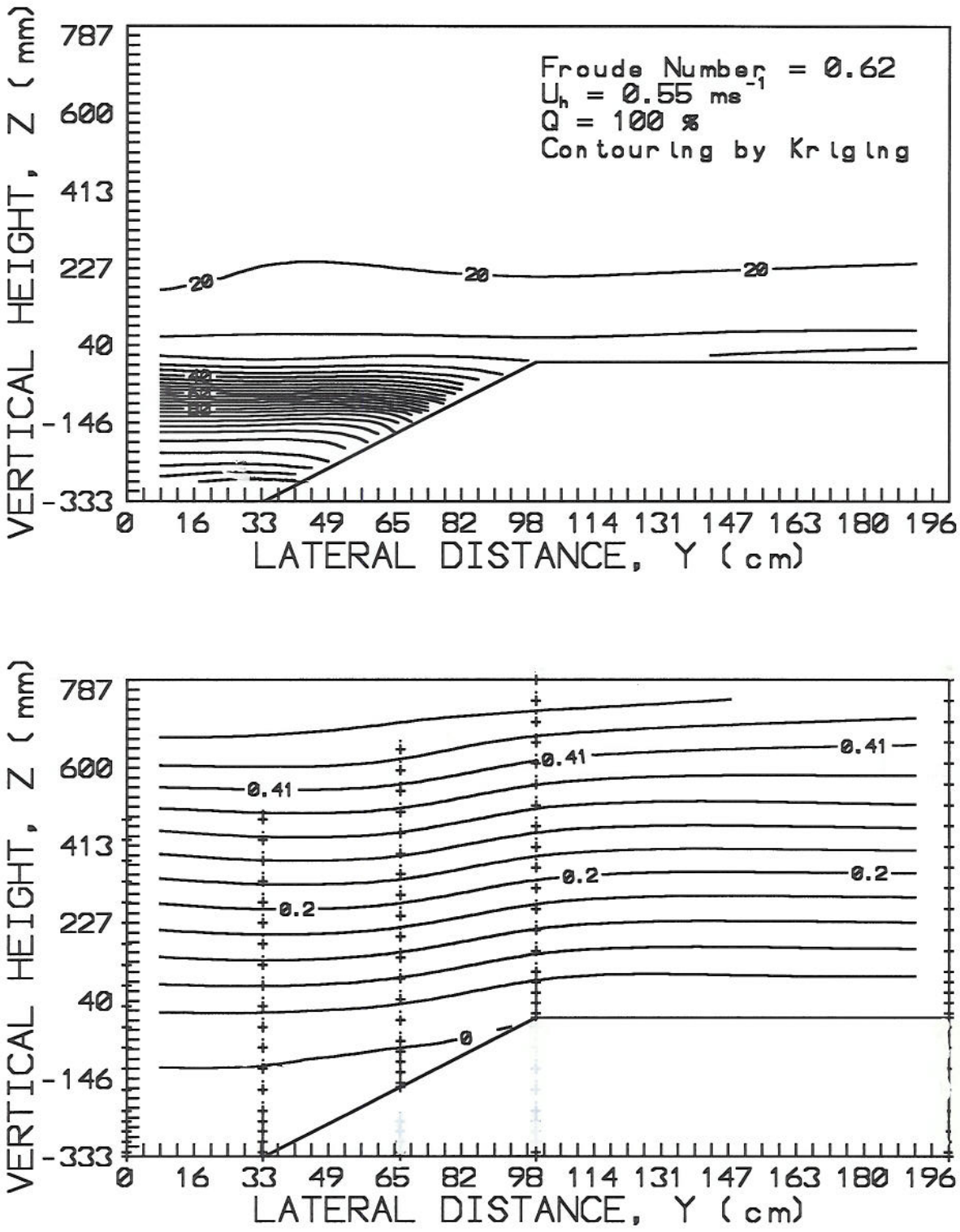

Fig. 12 Lateral isotherm (°C) and streamline contours (m^2/s) above open-pit mine model. Fr = 0.62. Measurement locations noted by +.

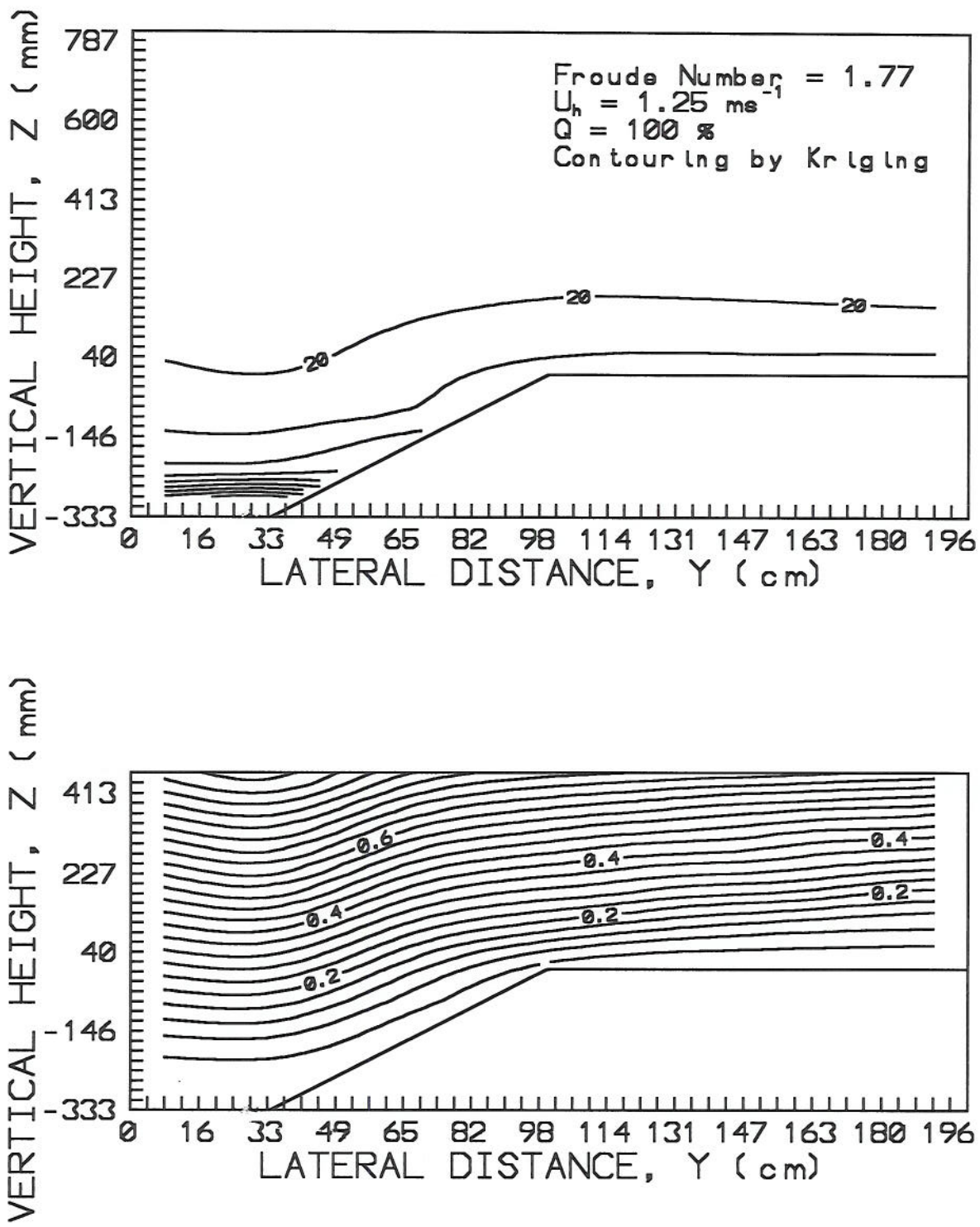

Fig. 13 Lateral isotherm (°C) and streamline (m^2/s) contours over open-pit mine model. Fr = 1.77.

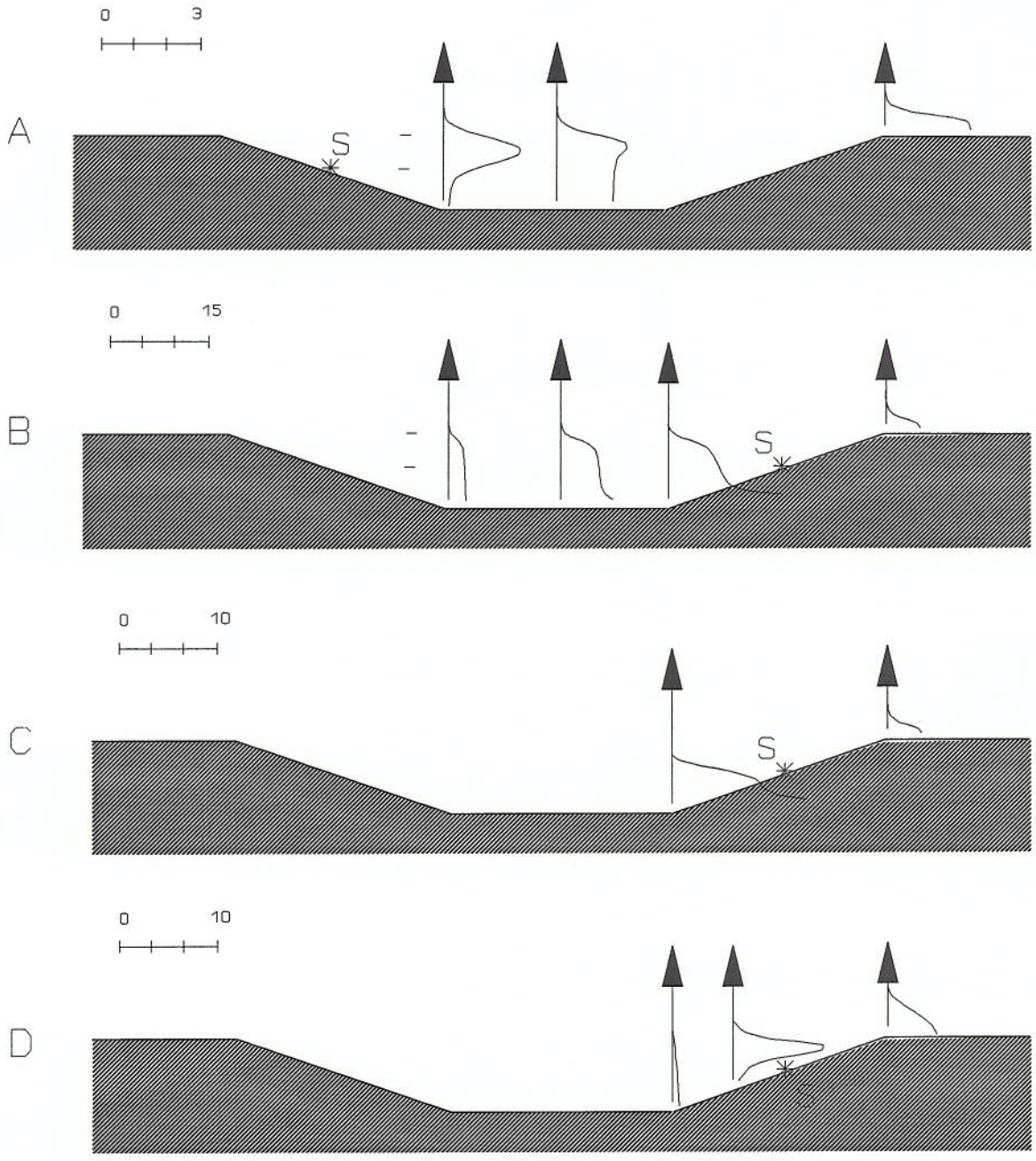

Fig. 14 Vertical concentration profiles measured over model open-pit coal mine. Pit Froude numbers during measurements are (A) 0.62, (B) 0.62, (C) 0.67 and (d) 1.09.

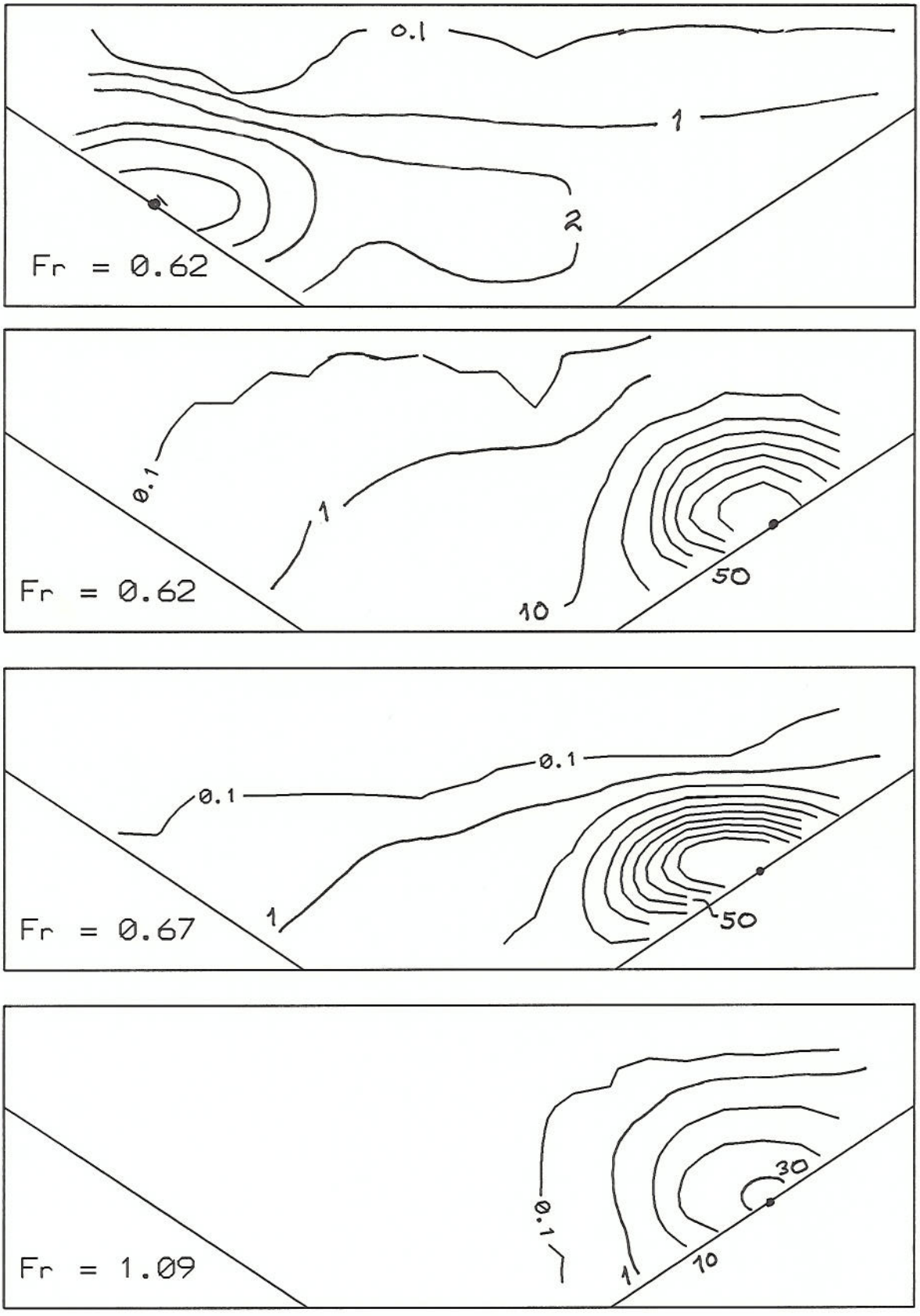

Fig. 15 Contours of concentration (ppt) for release configurations noted in previous figure.